

## Testing the Pauli exclusion principle with the NEMO-2 detector

R. Arnold<sup>11</sup>, C. Augier<sup>9</sup>, J. Baker<sup>5</sup>, A. Barabash<sup>8</sup>, D. Blum<sup>9</sup>, V. Brudanin<sup>3</sup>, A.J. Caffrey<sup>5</sup>, J.E. Campagne<sup>9</sup>, E. Caurier<sup>11</sup>, D. Dassié<sup>1</sup>, V. Egorov<sup>3</sup>, T. Filipova<sup>3</sup>, R. Gurriaran<sup>1</sup>, J.L. Guyonnet<sup>11</sup>, F. Hubert<sup>1</sup>, Ph. Hubert<sup>1</sup>, S. Jullian<sup>9</sup>, O. Kochetov<sup>3</sup>, I. Kisel<sup>3</sup>, V.N. Kornoukhov<sup>8</sup>, V. Kovalenko<sup>3</sup>, D. Lalanne<sup>9</sup>, F. Laplanche<sup>9</sup>, F. Leccia<sup>1</sup>, I. Linck<sup>11</sup>, C. Longuemare<sup>2</sup>, Ch. Marquet<sup>1</sup>, F. Mauger<sup>2</sup>, H.W. Nicholson<sup>10</sup>, I. Pilugin<sup>8</sup>, F. Piquemal<sup>1</sup>, J-L. Reyss<sup>4</sup>, X. Sarazin<sup>9</sup>, F. Scheibling<sup>11</sup>, J. Suhonen<sup>6</sup>, C.S. Sutton<sup>10</sup>, G. Szklarz<sup>9</sup>, V. Timkin<sup>3</sup>, R. Torres<sup>1</sup>, V.I. Tretyak<sup>7</sup>, V. Umatov<sup>8</sup>, I. Vanyushin<sup>8</sup>, A. Vaille<sup>1</sup>, Yu. Vasilyev<sup>7</sup>, Ts. Vylov<sup>3</sup>

<sup>1</sup> CENBG, IN2P3-CNRS et Université de Bordeaux, 33170 Gradignan, France

<sup>2</sup> LPC, IN2P3-CNRS et Université de Caen, 14032 Caen, France

<sup>3</sup> JINR, 141980 Dubna, Russia

<sup>4</sup> CFR, CNRS, 91190 Gif sur Yvette, France

<sup>5</sup> INEEL, Idaho Falls, ID 83415, USA

<sup>6</sup> JYVÄSKYLÄ University, 40351 Jyväskylä, Finland

<sup>7</sup> INR, 252028 Kiev, Ukraine

<sup>8</sup> ITEP, 117259 Moscow, Russia

<sup>9</sup> LAL, IN2P3-CNRS et Université Paris-Sud, 91405 Orsay, France

<sup>10</sup> MHC, South Hadley, Massachusetts 01075, USA

<sup>11</sup> IN2P3-CNRS et Université Louis Pasteur, 67037 Strasbourg, France

Received: 25 August 1999

Communicated by B. Povh

**Abstract.** The Pauli Exclusion Principle (PEP) was tested with the NEMO-2 detector. Limits at the 90% C.L. on the violation of PEP for p-shell nucleons in  $^{12}\text{C}$  were obtained. Specifically, transitions to the fully occupied  $1s_{1/2}$ -shell yielded a limit of  $4.2 \cdot 10^{24}$  y for the process with emission of a  $\gamma$ -quantum. Similarly limits of  $3.1 \cdot 10^{24}$  y for  $\beta^-$  and  $2.6 \cdot 10^{24}$  y for  $\beta^+$  Pauli-forbidden transitions of  $^{12}\text{C} \rightarrow ^{12}\tilde{\text{N}}(^{12}\tilde{\text{B}})$  are reported here.

**PACS.** 23.90.+w Other topics in radioactive decay and in-beam spectroscopy – 11.30.Ly Other internal and higher symmetries

### 1 Introduction

The Exclusion Principle is one of the most fundamental laws of nature. It was formulated by W. Pauli in 1925 [1] to explain the regularities of the Periodic Table of elements and the characteristic features of atomic spectra. In modern Quantum Field Theory (QFT) the Exclusion Principle appears automatically from the nature of identical particles and the anti-commutativity of the fermion creation (annihilation) operators. It postulates that in a system of identical fermions, two or more particles cannot occupy the same state.

The discovery in 1956 of parity non-conservation in  $\beta$ -decay [2] showed for the first time that “fundamental laws” can be violated. The violation of CP invariance was then discovered in 1964 [3]. As a result, all conservation laws began to be tested. Some of them, for example the non-conservation of leptonic and barionic quantum numbers can be explained in the framework of models satisfying all the principles of standard QFT. Others, such as the non-

conservation of the electric charge [4–7], CPT-violation [8,9], and Lorentz-invariance violation [10,11], require a global reconstruction of modern theoretical physics to create self-consistent models.

As indicated by L.B. Okun [12], a non-conformist approach to the Pauli Exclusion Principle (PEP) could be traced to remarks by P.A.M. Dirac, W. Pauli and E. Fermi. Carefully reading the famous book by Dirac [13], one can conclude that in the framework of QFT with a Hamiltonian, which is permutationally invariant, transitions to a filled shell are forbidden independent of the validity of the Pauli Principle. Such transitions would change the permutational symmetry of the wave function of a given set of particles.

In 1934 E. Fermi discussed in one of his popular science articles [14] the possibility that electrons are a “little bit” non-identical. He predicted that a tiny variation would drastically change the properties of atoms during the billions of years of their existence.

In model [15] the electron presents a superposition of a large number of almost degenerated mass eigenstates. Thus the properties of the electron changes slightly with time. Critical remarks to this idea can be found in the literature [16].

In more recent publications [17–21, 12] some attempts were made to introduce into the theory a small violation of PEP, but they have not been successful. PEP is at the heart of the QFT and its violation, even if very small, leads to the appearance of states with negative norma (negative probability) [22, 23]. Thus there is no answer to the question, “What is the accuracy of PEP?”. The reason for this is that there is no real self-consistent and non-contradictory model, with small PEP violation. Indeed any model with PEP violation must be beyond the standard QFT. It was L.B. Okun [12, 18], who said, “That exceptional place occupied by the Pauli principle in modern physics does not imply that it does not need further painstaking experimental tests. Quite the opposite: the fundamental character of this principle generates special interest to its quantitative testing throughout the Mendeleev Table”.

There are two types of experiments to test PEP violation. The first is the search for atoms or nuclei in a non-Paulian state. The second is the search for evidence of transitions of atoms and nuclei into a non-Paulian state. In this article we consider the second process, with the PEP-violation in nuclei.

In 1979 testing of PEP was carried out in a search for  $\gamma$ -quanta (energy  $\sim 20$  MeV), which would accompany the transition of a nucleon from the  $2p$ - to the filled  $1s$ -shell of  $^{12}\text{C}$  nucleus. A lower limit was reported for the time of that transition,  $T_{1/2} > 2 \cdot 10^{20}$  y [25]. Using the experimental data of LSD, the limit on the  $\beta^- (\beta^+)$ -transition of the  $^{12}\text{C}$  into an anomalous state of  $^{12}\tilde{\text{N}} (^{12}\tilde{\text{B}})$  was extracted,  $T_{1/2} > 3 \cdot 10^{27}$  y [27]. In 1980 R. Amado and H. Primakoff [24] came to the conclusion, that in the framework of QFT, PEP-forbidden transitions [25] do not take place even if there is a PEP-violation. Their argument centered around the anti-symmetry of wave functions of identical fermions and permutation symmetry of the system Hamiltonian. A second argument was adduced in [26] for the results of the LSD data [27]. As mentioned above, no PEP-violating theory can be constructed from the standard hypothesis of QFT. In any case, experiments carry out tests on the fundamental principles of QFT, the identity of the particles and the connection of spin-statistics, as expressed by half-life limits on its violation. Here we talk about testing of PEP for historical reasons only. It doesn't matter that there are no consistent theories with the PEP-violation. Experiments have the advantage that any direct indication would have catastrophic implications for current theoretical models.

Presented are limits on anomalous PEP-violating transitions in  $^{12}\text{C}$  as extracted from the experimental data of the NEMO-2 detector.

## 2 NEMO-2 detector

The NEMO-2 detector [28] was designed for double beta decay studies and operated in the Fréjus Underground Laboratory (4800 m w.e.) from 1991 to 1997. During this period, the two neutrino double beta decays of  $^{100}\text{Mo}$  [29],  $^{116}\text{Cd}$  [30],  $^{82}\text{Se}$  [31] and  $^{96}\text{Zr}$  [32] were investigated in detail through the measurements of the summed electron energy spectra, angular distributions and single electron spectra.

### 2.1 Short description

The NEMO-2 detector (Fig. 1) consisted of a  $1\text{m}^3$  tracking volume filled with a mixture of helium gas and 4% ethyl alcohol. Vertically bisecting the detector was the plane of the source foil under study ( $1\text{m} \times 1\text{m}$ ). Tracking was accomplished with long, open Geiger cells with an octagonal cross section defined by  $100 \mu\text{m}$  nickel wires. On each side of the source foil there were 10 planes of 32 cells which alternated between vertical and horizontal orientations. Collectively, the cells provide three-dimensional tracking of charged particles.

A calorimeter made of scintillators covered two vertical opposing sides of the tracking volume. It consisted of two planes of 25 scintillators ( $19\text{cm} \times 19\text{cm} \times 10\text{cm}$ ), combined with low radioactivity photomultiplier tubes (PMT).

The tracking volume and scintillators were surrounded by a lead (5 cm) and iron (20 cm) shield for measurements with  $^{100}\text{Mo}$  and  $^{116}\text{Cd}$ . The same shield was used in the experiment with  $^{82}\text{Se}$  and  $^{96}\text{Zr}$  foils for 6222.6 h with the Zr foils placed at the central part of the source plane. The lead was then placed outside the iron for 1784.5 h. Next, the lead was removed for 536 h. At the end, 15 cm of paraffin was installed outside of the iron for the final 2162.8 h.

### 2.2 Performances

Details of the performance and parameters are described elsewhere [28], while the most salient characteristics are outlined briefly here. Three-dimensional measurements of charged particle tracks are provided by the array of Geiger cells. The transverse position is given by the drift time, and the longitudinal position is given by the plasma propagation times. The transverse resolution is  $500 \mu\text{m}$  and the longitudinal resolution is 4.7 mm. The calorimeter's energy resolution (FWHM) is 18% at 1 MeV with a time resolution of 275 ps (550 ps at 0.2 MeV). Scintillation counters measured the energy of an individual electron in the interval from 50 keV to 4 MeV. Electrons with energies near or above 4 MeV may fall into the “saturation” regime of the counters. More specifically,  $E_{sat}$  is different for each counter and varies from 4 to 7 MeV. The only information for events in this regime is that they have a deposited energy higher than  $E_{sat}$ . A laser and fiber optics device is used to check the stability of the scintillation detectors.

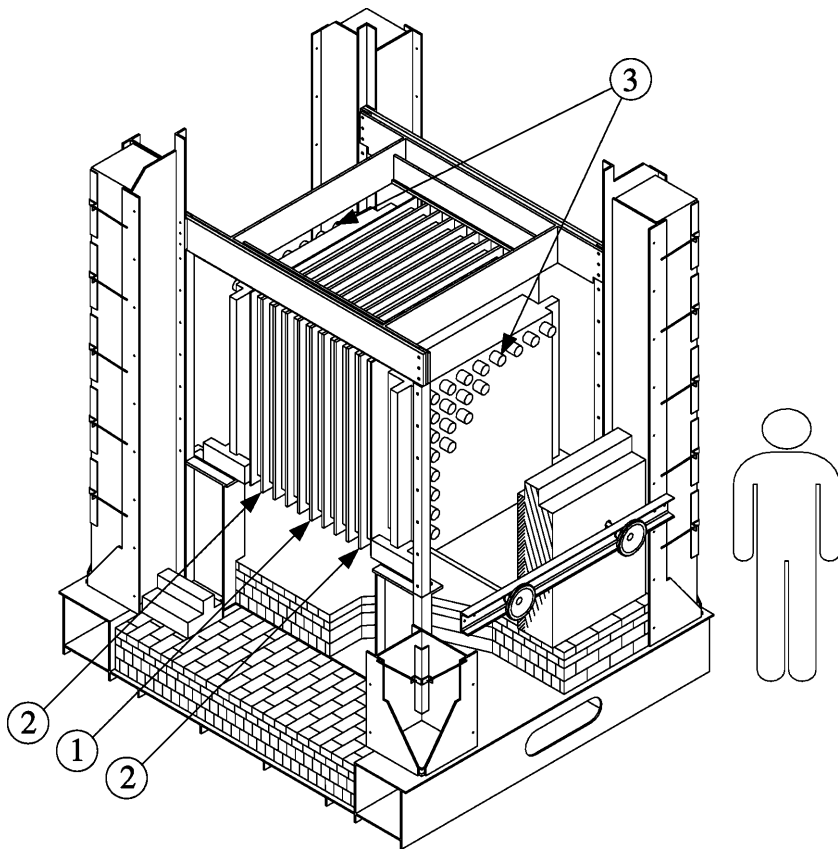


**Fig. 1.** The NEMO-2 detector without shielding. (1) Central frame with the source plane capable of supporting plural source foils. (2) Tracking device of 10 frames, each consisting of two perpendicular planes of 32 Geiger cells. (3) Two scintillator arrays each consisting of 5 by 5 counters. In the earlier experiment with molybdenum sources [29] the scintillator arrays were 8 by 8 counters as depicted here

A trigger requiring one or two scintillation counters and four Geiger frames normally runs at a rate of 0.01–0.04 Hz depending on the radon levels in the laboratory. This trigger rate is too low for an efficient calibration survey of the experiment, so a second trigger requiring only one counter with an energy greater than 1.3 MeV was added.

### 2.3 Event definition

An electron is defined by a track linking the source foil and one scintillator. The maximum scattering angle along the track has to be less than  $20^\circ$  to reject hard scattering situations. A photon is recognized as one or two adjacent-fired scintillators, without an associated particle track. For photons and electrons, an energy deposited greater than 200 keV is required in order to obtain sufficiently good time resolution for time-of-flight analysis of events. The two-electron events are defined by two tracks which have a common vertex in the source foil and are associated with two fired scintillators. More detailed description can be found in the following references [28–31].

## 3 Experimental results

The NEMO-2 detector’s experimental data from measurements with Cd, Se and Zr foils were used to estimate limits

on non-Paulian transitions in the  $^{12}\text{C}$  of the plastic scintillators. The total mass of  $^{12}\text{C}$  under study was 170 kg.

Figure 2 shows non-Paulian transitions in  $^{12}\text{C}$ . In Fig. 2a, the transition of a nucleon from the  $p$ -shell to the fully occupied  $1s_{1/2}$ -shell is shown. This process is accompanied by  $\gamma$ -quantum emission, where its energy equals the energy difference between the  $p$  and  $s$  levels ( $\sim 20$  MeV) [25]. In subsequent figures, (Fig. 2b,c), the  $\beta^\pm$  transitions of  $^{12}\text{C}$  to non-Paulian  $^{12}\text{B}$  and  $^{12}\text{N}$  are shown when a nucleon falls from the  $p$ -shell to the fully occupied  $1s_{1/2}$ -shell. The emitted  $\beta^+$  or  $\beta^-$  are distributed as ordinary  $\beta$ -decay spectra with an endpoint energy 20 MeV [27]. Cuts were used for extracting fine limits from the experiment.

### 3.1 Non-Paulian processes with high energy $\gamma$ -quantum emission

High energy  $\gamma$ -quanta produced in scintillator of the non-Paulian transition to  $^{12}\text{C}$  were considered. The  $\gamma$ -quanta cross the tracking volume, interact with a source foil and give two tracks and two fired scintillators. In the energy region  $E_\gamma \sim 20$  MeV, pair creation probability in the source foil ( $45\text{--}50$  mg/cm $^2$ ), is higher by 2–3 orders of magnitude than those for double Compton interactions or Möller scattering of Compton electrons in the foil. The NEMO-2 detector was not designed to distinguish between  $e^+$  and  $e^-$  tracks, thus pairs were detected as two electron events (2e). A time-of-flight analysis was used to select high energy 2e events in both simulation and experimental data.

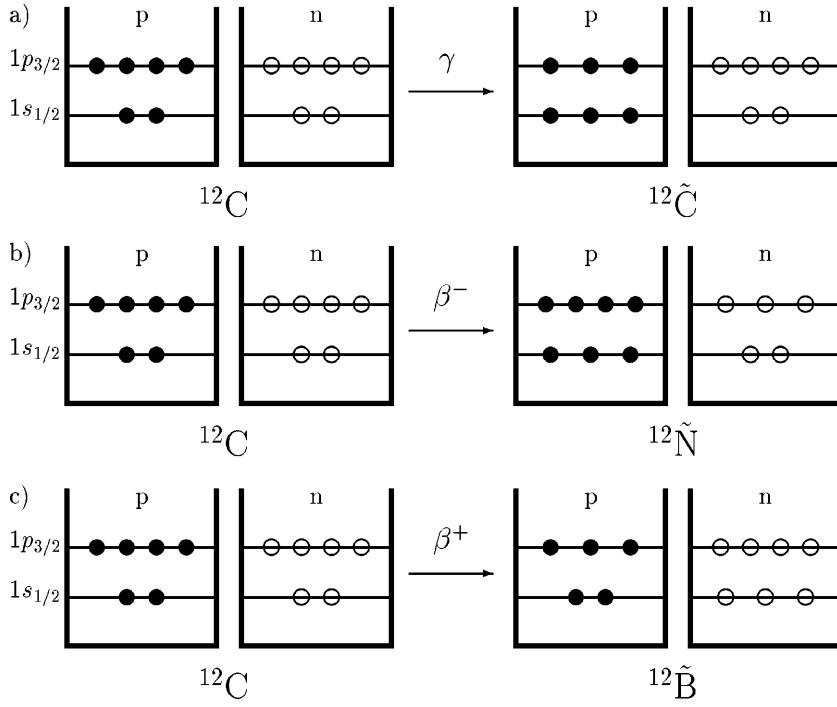


**Fig. 2.** Schemes of non-Paulian transitions in  $^{12}\text{C}$ . (a) transition of a proton from the  $p$ -shell to the fully occupied  $s$ -shell (a similar figure can be constructed for neutrons) (b) non-Paulian  $\beta^-$  transition of  $^{12}\text{C}$  to  $^{12}\tilde{\text{N}}$ ; (c) non-Paulian  $\beta^+$  transition of  $^{12}\text{C}$  to  $^{12}\tilde{\text{B}}$

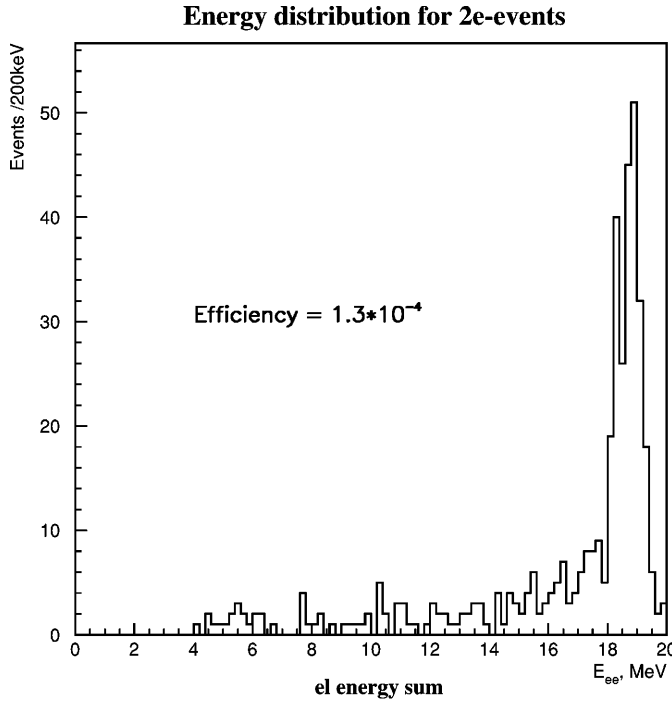


**Fig. 3.** Simulated summed electron energy spectrum of two electron events coming from the source foil for which the event was generated by a 20 MeV  $\gamma$ -quanta in the plastic scintillators. A cut at 4 MeV is applied

The simulated data studied  $3.8 \cdot 10^6$  events with initial  $\gamma$ -quanta emitted from the scintillators. The maximum in the summed electron energy ( $E_{2e}$ ) spectrum (Fig. 3) is at the energy of  $\gamma$  minus two electron's masses.

No events with two tracks and summed energy  $\geq 4$  MeV were found in the experiment with Se and Zr given an exposure of 10357 h [31,32] and in the enriched Cd measurement with an exposure of 6588 h [30]. The detection efficiency for  $E_{2e} \geq 4$  MeV and  $\cos(\theta_{2e}) > 0$  is equal to 0.013% for the Se-Zr source. In the case of the enriched Cd the efficiency should be scaled by a factor of 0.57 because of enriched Cd is another material with different thickness and has occupied only a half of the source plane. From these data one can obtain a limit on the PEP-violated transition of  $^{12}\text{C}$  nucleus to  $^{12}\tilde{\text{C}}$  at the 90% C.L.:

$$T_{1/2} > 5.3 \cdot 10^{23} \text{y.}$$

Next the limit on PEP violating transitions of nucleons from the  $p$ -shell to the fully occupied  $1s_{1/2}$ -shell in  $^{12}\text{C}$  at the 90% C.L. is:

$$T_{1/2} > 4.2 \cdot 10^{24} \text{y.}$$

### 3.2 $\beta^\pm$ decays to non-Paulian states

The search for  $\beta^\pm$  decay processes were performed through the selection of two tracks events. Cuts for these events require an electron to appear in a plastic scintillator, cross the tracking volume and source plane and then enter a plastic scintillator on the opposite side of the NEMO-2 detector. Simulation of  $\beta^+$  and  $\beta^-$  decays of  $^{12}\text{C}$  to non-Paulian states of daughter nuclei in plastic scintillators was thus examined. The simulated spectra are presented in Fig. 4. Evident here is that the efficiency for  $\beta^+$  decays is lower in comparison to  $\beta^-$  decays because the detection of at least one annihilation  $\gamma$ -quantum (511 keV) leads to the rejection of such an event.

**Table 1.** Limits on the non-Paulian transitions in  $^{12}\text{C}$ 

| Channel                    | $\gamma$ emission       | $\beta^-$ decay         | $\beta^+$ decay         |
|----------------------------|-------------------------|-------------------------|-------------------------|
| Window (MeV)               | [4,20]                  | [4,20]                  | [4,20]                  |
| Number of events           | 0                       | 1                       | 1                       |
| Efficiency                 | $1.3 \cdot 10^{-4}$     | $8.5 \cdot 10^{-3}$     | $7.2 \cdot 10^{-3}$     |
| $T_{1/2}$ (90% CL) present | $> 4.2 \cdot 10^{24}$ y | $> 3.1 \cdot 10^{24}$ y | $> 2.6 \cdot 10^{24}$ y |
| $T_{1/2}$ (99.7% CL) [25]  | $> 1.3 \cdot 10^{20}$ y |                         |                         |
| $T_{1/2}$ (90% CL) [27]    |                         | $> 8 \cdot 10^{27}$ y   | $> 8 \cdot 10^{27}$ y   |

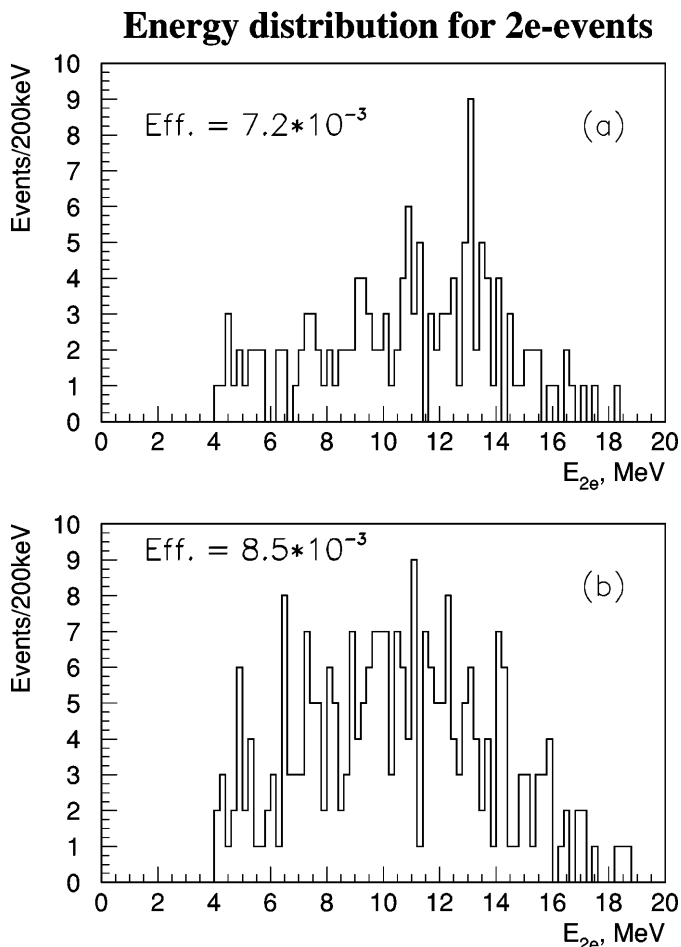


**Fig. 4.** Energy spectra of simulated two track events: (a) for  $\beta^+$  decay and (b) for  $\beta^-$  decay of  $^{12}\text{C}$  to non-Paulian states of daughter nuclei with a 20 MeV endpoint energy. A cut at 4 MeV is applied for comparison with the experimental data

The main background in the energy range up to 8 MeV is due to neutrons from natural sources. Consequently the data used here was obtained in a run with a paraffin shield (2162.8 h), which efficiently suppressed the neutron background. Only one event with summed energy deposit of  $E > 4$  MeV was found in the experiment involving Se and Zr samples. The detection efficiency of  $\beta^-$  is equal to 0.85% , and for  $\beta^+$  is 0.72%. As a result, one can ob-

tain limits on  $\beta^\pm$  decays of  $^{12}\text{C}$  to non-Paulian states of daughter nuclei  $^{12}\text{B}$  and  $^{12}\text{N}$  at the 90% C.L.:

$$T_{1/2} > 3.1 \cdot 10^{24} \text{ y} \quad \text{for } \beta^-$$

and

$$T_{1/2} > 2.6 \cdot 10^{24} \text{ y} \quad \text{for } \beta^+.$$

#### 4 Discussion and conclusion

Table 1 presents the NEMO-2 results on non-Paulian transitions in  $^{12}\text{C}$ . Due to good time-of-flight selection and a large mass of plastic scintillators, the limits for 20 MeV gamma emission is higher by four orders of magnitude than the previous limit [25]. Limits on the  $\beta^\pm$  non-Paulian transitions are lower than in [27], because of the relative small masses involved and the low efficiency for crossing electron detection.

The new detector, NEMO-3, which is under construction now [33], will help to improve these limits. The amount of  $^{12}\text{C}$  will be  $\sim 40$  times greater and the detection efficiency 10 times higher. Additionally a magnetic field will be applied to distinguish  $e^+e^-$  events from  $e^-e^-$ . So expected limits which will be obtained with the NEMO-3 detector will be 3 or 4 orders of magnitude higher or PEP violating transitions will be observed.

The authors would like to thank the Fréjus Underground Laboratory staff for their technical assistance in running the experiment. The authors are also thankful to L.B. Okun for a very fruitful discussion. The portions of this work conducted in Russia were supported by RFBR grant number 97-02-17344 and by INTAS grant 96-0589.

#### References

1. W. Pauli, Z.Phys. **31**, (1925) 765
2. C.S. Wu, E. Ambler, R.W. Hayward et al., Phys. Rev. **105** (1957) 1413
3. J.H. Christinsen, J.W. Cronin, V.L. Fitch et al., Phys. Rev. Lett. **13** (1964) 138
4. L.B. Okun, Ya.B. Zeldovich, Phys. Lett. **78B** (1978) 597
5. A.Yu. Ignatiev, V.A. Kuzmin, M.E. Shaposhnikov, Phys. Lett. **B84** (1979) 315
6. M.B. Voloshin, L.B. Okun, JETP Lett. **28** (1978) 145

7. R.N. Mohapatra, S. Nussinov, *J.Mod.Phys.* **A7** (1992) 3817
8. J. Ellis, N.E. Mavromatos, D.V. Nanopoulos, *Proc. Int. Workshop on K Physics, Ed. Lydia Iconomidou-Fayard* (Editions Frontieres, Orsay, France, 1997) 187
9. V.A. Kostelecky, *ibid*, 407
10. H.B. Nielsen, M. Ninomiya, *Nucl. Phys.* **B141** (1978) 153
11. V.A. Kostelecky, S. Samuel, *Phys. Rev.* **D39** (1989) 683
12. L.B. Okun, *Sov.Phys.Usp.* **32** (1989) 543
13. P.A.M. Dirac, *The Principles of Quantum Mechanics* (Clarendon Press, Oxford 1958) Ch. IX
14. E. Fermi, *Atti. Sci. If Progr. Sci. 22 Riunione* **3** (Bari 1933) 7; *Scientia* **55** (1934) 21
15. V.L. Luboshits, M.I. Podgoretsky, *ZhETF* (in Russian) **60** (1971) 9
16. I.Yu. Kobzarev, N.N. Nikolaev, L.B. Okun, *ZhETF* (in Russian) **10** (1969) 864
17. A.Yu. Ignatiev, V.A. Kuzmin, *Sov. Journ. Nucl. Phys.* **56** (1987) 444
18. L.B.Okun, *JETP Lett.* **46** (1987) 529
19. O.W. Greenberg, R.N. Mohapatra, *Phys. Rev. Lett.* **59** (1987) 2507
20. O.W. Greenberg, R.N. Mohapatra, *Phys. Rev.* **D39** (1989) 2032
21. O.W. Greenberg, R.N. Mohapatra, *Phys. Rev. Lett.* **62** (1989) 712
22. A.B. Govorkov, *Phys. Lett.* **A137** (1989) 7
23. A.B. Govorkov, preprint JINR **E2-90-364** (1990)
24. R.D. Amado, H. Primakoff, *Phys. Rev.* **C22** (1980) 1338
25. Logan B.A. and Ljubicic, *Phys. Rev.* **C20** (1979) 1957
26. T.Sudbery, *Nature* **348** (1990) 193
27. Kekez D., Ljubicic A. and Logan B.A., *Nature* **348** (1990) 224
28. R. Arnold et al., *Nucl. Instr. Meth.* **A354** (1995) 338
29. D. Dassié et al., *Phys. Rev.* **D51** (1995) 2090
30. R. Arnold et al., *Z. Phys.* **C72** (1996) 239
31. R. Arnold et al., *Nucl. Phys.* **A636** (1998) 209
32. R. Arnold et al., submitted to *Nucl. Phys. A*
33. NEMO-3 Proposal, preprint LAL **94-29** (1994)